HHS Public Access

Author manuscript

Obesity (Silver Spring). Author manuscript; available in PMC 2018 September 22.

Published in final edited form as:

Obesity (Silver Spring). 2018 May ; 26(5): 885–894. doi:10.1002/oby.22166.

Inherently lean rats have enhanced activity and skeletal muscle response to central melanocortin receptors

Chaitanya K. Gavini[1,2], **Steven L. Britton**[3,4], **Lauren G. Koch**[3,6], and **Colleen M. Novak**[1,5]

[1]School of Biomedical Sciences, Kent State University, Kent, Ohio, USA

[2]Department of Cell and Molecular Physiology, Stritch School of Medicine, Loyola University Chicago, Maywood, Illinois, USA

[3]Department of Anesthesiology, University of Michigan, Ann Arbor, Michigan, USA

[4]Department of Molecular and Integrative Physiology, University of Michigan, Ann Arbor, Michigan, USA

[5]Department of Biological Sciences, Kent State University, Kent, Ohio, USA

[6]Department of Physiology and Pharmacology, The University of Toledo College of Medicine and Life Sciences, Toledo, Ohio, USA

Abstract

Objective—Activity thermogenesis and energy expenditure (EE) are elevated in intrinsically lean rats (high-capacity runners, HCR), and are also stimulated by melanocortin receptor activation in the ventromedial hypothalamus (VMH). Here, we determined if HCR are more responsive to central modulation of activity EE compared to low-capacity runners (LCR).

Methods—HCR and LCR rats received intra-VMH microinjections of Melanotan II (MTII), a mixed melanocortin receptor agonist. Changes in EE, respiratory exchange ratio (RER), activity EE, muscle heat, norepinephrine turnover (NETO), and muscle energetic modulators were compared.

Results—HCR were significantly more responsive to intra-VMH MTII-induced changes in EE, activity EE, NETO to some muscle subgroups, and muscle mRNA expression of some energetic modulators. Though HCR had high muscle activity thermogenesis, limited MTII-induced modulation of muscle thermogenesis during activity was seen in LCR only.

Conclusions—An inherently lean, high-capacity rat phenotype showed elevated response to central melanocortin stimulation of activity EE and use of fat as fuel. This may be driven by sympathetic outflow to skeletal muscle, which was elevated after MTII. Central melanocortin

Correspondence should be addressed to Chaitanya K. Gavini, Department of Cell and Molecular Physiology, Stritch School of Medicine, Loyola University Chicago, 2160 S. First Ave, Maywood, IL 60153, USA. Tel: +1 708 216 7936; cgavini@luc.edu.

Disclosure:
The authors declare no conflict of interest.

receptor activation also altered skeletal muscle energetic modulators in a manner consistent with elevated EE and lowered RER.

Keywords

High- and low-capacity runners (HCR. LCR); energy expenditure; obesity; skeletal muscle

INTRODUCTION

Genetic and environmental factors interact to influence energy balance. One characteristic that differs with leanness is physical activity, a heritable trait that varies widely between individuals in both humans and rodents[1,2,3]. Across species, intrinsic aerobic capacity predicts high physical activity, health, longevity, and a favorable metabolic profile[4,5,6,7,8,9,10,11]. Rats selectively bred as high capacity runners (HCR) are more physically active than their counterparts selectively bred as low capacity runners (LCR). LCR are prone to weight gain, obesity, and cardiovascular disorders[6,12], and HCR have a low adiposity, high activity (independent of differences in body weight[13]), and high energy expenditure (EE) relative to body size[13]. The high EE seen in HCR is predominantly due to heightened non-resting EE[13], which persists even during controlled activity, indicating low economy of activity—more kcal used for the same workload—in the HCR[12,13]. This implicates skeletal muscle energetic and thermogenic mechanisms, which may stem from the enhanced sympathetic drive observed in HCR[13].

The elevated activity, EE, SNS drive, and muscle expression of energetic mediators characteristic of HCR are also modulated by central melanocortin receptors[14,15,16], suggesting a melanocortinergic mechanism for the muscle energetic phenotype of HCR. Like brain melanocortins, the ventromedial hypothalamus (VMH) plays an important role in fuel allocation[15,16,17,18]. Activation of VMH melanocortin receptors using a non-specific agonist Melanotan II (MTII) increases EE and physical activity, and decreases respiratory exchange ratio (RER), switching fuel preference to fats; it lowers fuel economy during activity where ‘wasted’ calories are dissipated as heat[14]. HCR and LCR respond differently to central melanocortins[19,20], a system known to modulate sympathetic drive[15,16,21]. Here, we examine how VMH melanocortin receptors alter activity-related EE, heat dissipation, SNS drive, and molecular mediators of energy homeostasis in lean (HCR) and obesity-prone (LCR) rats, predicting that increased EE and thermogenesis will be reflected in augmented activation at each level of this brain-muscle pathway.

METHODS

Adult male HCR-LCR rats (N=104, 52-group, generation 32 and 34) from the University of Michigan were individually housed on a 12:12 light:dark cycle (lights on at 0700 EST) and received food (5P00 MRH 3000) and water *ad libitum*. All studies were approved by the Kent State University IACUC.

Stereotaxic surgery and transponder implantation

Stereotaxic surgeries were performed to chronically implant guide cannulae aimed at the VMH[14]. Briefly, rats (total N=86 for cannulation) were anesthetized using isoflurane and mounted on a stereotaxic apparatus using atraumatic ear bars. The VMH was targeted using the coordinates: anterior-posterior, −2.5mm; medial-lateral, +0.5mm; dorsal-ventral, −6mm (from dura), and an injection needle with 3mm projection (final dorsal-ventral, −9mm from dura). After completion of the study, rats with guide cannulae within 250μm of the VMH (N=74 accurate placements) were used for data analysis as shown in our previous studies[14,20]. In 24 male HCR-LCR (12/group) during stereotaxic surgery, sterile IPTT-300 temperature transponders (Bio Medic Data Systems, Inc.) were implanted on interscapular brown adipose tissue (BAT) and adjacent to gastrocnemius muscle bilaterally.

Body composition and energy expenditure

Body composition was measured using an EchoMRI-700 (EchoMRI, Houston, TX) to determine the fat and lean mass (in grams) of each rat the day before experiments. This did not interfere with transponder function. After 24–48hrs of acclimation in testing cages, EE and physical activity were measured using small-animal indirect calorimetry (4-chamber Oxymax FAST system, Columbus Instruments, Columbus, OH) at thermoneutral conditions, as previously reported[13,14]. Rats were injected either with the nonspecific melanocortin receptor agonist MTII (20pmoles/200nl) or vehicle (aCSF, 200nl)[14]. The first 15 min of data was not included in the analysis. EE data (VO_2, VCO_2, RER, kcal/hr) were averaged, and physical activity data were expressed as mean beam breaks/minute. In all EE and thermogenesis studies described here, all rats received counterbalanced vehicle and MTII injections separated by at least four days, with each rat acting as its own control thereby nullifying the effect of body weight and composition[22,23]. For EE, analysis of covariate was used to account for differences in body composition.

To assess locomotor efficiency, physical-activity EE was measured using gas exchange during a treadmill activity test; MTII-induced physical activity precluded accurate measurement of resting EE. At least one day after a 15-min treadmill acclimation period, rats were placed in the treadmill after injections of either MTII (20pmoles/200nl) or vehicle (aCSF) and allowed to acclimate without food for 2 hrs. Rats then walked on the treadmill at 7 m/min for 30 min while activity-EE data were collected every 10 sec. All EE data from both studies were analyzed using 2×2 mixed ANOVA using SPSS, with ANOVA significance set at $p < 0.05$ unless otherwise stated.

Muscle temperature

Skeletal muscle and BAT heat dissipation were measured every 15 min for 4 hrs after intra-VMH MTII or vehicle microinjection, with BAT thermogenesis as a positive control. In a separate experiment, rats received microinjections of either MTII or vehicle 1.5 hrs prior to measurement of skeletal muscle heat dissipation during controlled physical activity on a treadmill. Gastrocnemius temperatures in each leg were recorded at baseline (before injecting and immediately before treadmill walking) and at set intervals during a 35-min, 5-level graded treadmill test as reported previously[13,14]. Data from each study were analyzed using 3-way ANOVAs.

Norepinephrine turnover (NETO)

Norepinephrine (NE) turnover (NETO) was used to assess sympathetic drive to peripheral tissues including liver, heart, BAT, skeletal muscle (including quadriceps, lateral and medial gastrocnemius, EDL, and soleus), and WAT depots (mesenteric (MWAT), gluteal (GWAT), retroperitoneal (RWAT), inguinal (IWAT), and epididymal WAT (EWAT)) in HCR and LCR. NETO was measured using α-methyl-p-tyrosine (aMPT in saline vehicle) as previously reported[24,25]. HCR and LCR were divided into 3 groups (aMPT/MTII, aMPT/aCSF-vehicle, control; n=8/group). On the day of the study, food was removed and assigned rats were given aMPT injections (125 mg aMPT/kg body weight; 25 mg/ml) 2 and 4 hrs before tissue collection; 30 minutes after the first aMPT injection, rats received intra-VMH MTII or vehicle. All rats were euthanized by rapid decapitation between 1200 and 1500 EST (5–8 hrs after lights-on), 4 hours after the first aMPT injection. Tissues were rapidly dissected and snap-frozen in liquid nitrogen. Catecholamines were isolated from homogenized tissue and measured using HPLC, as previously described[13,14,24,25]. NETO was calculated:

$$k = (\lg[\mathrm{NE}]0 - \lg[\mathrm{NE}]4)/(0.434 \times 4)$$
$$\mathrm{K} = k[\mathrm{NE}]0$$

k is the constant rate of NE efflux (also known as fractional turnover rate),

[NE]0 is the initial NE concentration or from 0-hr group (control),

[NE]4 is the final NE concentration or from 4-hr group (aMPT-MTII/aMPT-vehicle), and K = NETO.

Differences in tissue NETO between intra-VMH MTII-microinjected and vehicle-microinjected rats were calculated with respect to control-group rats; NETO/gram tissue/hour was compared using a 2×2 mixed ANOVA.

mRNA and protein expression

Skeletal muscle (gastrocnemius and quadriceps), liver, MWAT, and BAT were collected from HCR/LCR rats (N=32, 16/group) 4hrs after intra-VMH microinjection of either MTII or vehicle (N=8/treatment). Tissue samples were homogenized and total mRNA extracted as previously reported[13,14], and compared to glyceraldehyde 3-phosphate dehydrogenase (GAPDH) using the comparative Ct method (ΔCt). See Supplementary Material for list of primers. Protein was isolated from tissue homogenate[13,14] and compared using Western blots. Primary and secondary antibodies (see Supplementary Material) were diluted in blocking buffer according to manufacturer instructions and developed using a chemiluminescence detector using an Amersham kit (GE Healthcare, UK). Data are expressed as a percent expression using samples from vehicle-treated HCR rats as the reference value (defined as 100%) relative to GAPDH (for mRNA) or actin (for protein), and were analyzed using 2×2 mixed ANOVA. As we were specifically interested in the magnitude of effect of MTII in HCR vs. LCR, we used planned *(a priori)* comparisons using t-tests with a Bonferroni correction (two t-tests with $p<0.025$).

RESULTS

For body weight and composition, LCR were consistently larger with more fat and lean mass than HCR. Some slight but significant differences were found between treatments (Table S1). Statistical results are listed in Tables S2–S16, with data expressed as mean ± SEM.

EE in HCR was more responsive to intra-VMH MTII

As shown in Figure 1A–D, intra-VMH MTII significantly increased EE, VO_2, and physical activity (horizontal and ambulatory), with a significantly greater response in HCR (significant interaction), and lowered RER in both HCR and LCR. HCR had higher activity (all dimensions), VO_2, and VCO_2. MTII also increased treadmill-activity EE and VO_2 (Figure 1E–H); MTII decreased RER more in LCR than HCR (Figure 1G). HCR showed a greater MTII-induced increase in treadmill-activity EE (Figure 1H). There were significant interactions between treatment and HCR/LCR for free-moving EE and treadmill-activity EE, using either body weight or lean mass as covariates. Treadmill-walking EE showed main effects where HCR had lower EE and RER, and a trend toward higher treadmill VO_2.

Muscle heat dissipation

As described in the Supplementary Material, during resting, compared to vehicle, MTII induced an increase in BAT temperature, and the change in temperature from baseline was significantly higher after MTII treatment (compared to vehicle) between 30min and 120min after injection (Figure S1). There were no significant differences in BAT response to MTII between HCR and LCR. Compared to vehicle, intra-VMH MTII did not significantly increase gastrocnemius muscle temperatures or elevation relative to baseline (Figure S2). Compared to vehicle injections, MTII injections induced higher treadmill activity-associated gastrocnemius temperatures in LCR (Figure 2A, B). Consistent with previous findings[13], lean HCR had a greater change in treadmill locomotion-induced skeletal muscle heat dissipation during treadmill locomotion under both vehicle- and MTII-injected conditions compared to obesity-prone LCR (Figure 2B).

Intra-VMH MTII microinjection differentially elevated sympathetic drive to metabolic tissues in lean vs. obesity-prone rats

Compared to vehicle, intra-VMH MTII induced a significant increase in SNS drive to skeletal muscle of both lean HCR and obesity-prone LCR, although HCR were significantly more affected (significant interaction) than LCR in soleus, quadriceps, and lateral gastrocnemius (Figure 3). Intra-VMH MTII also induced a significant increase in SNS drive to all WAT depots examined, BAT, heart, and liver (Figure 3, Table 1). MTII-induced NETO was greater in HCR than in LCR (significant interaction) for MWAT, GWAT, and IWAT, as well as for BAT and liver (Table 1). In heart, both baseline and MTII-induced NETO was greater in LCR than HCR, with a significant interaction where LCR showed a greater response to MTII (Figure 3F). Compared to vehicle-treated LCR, vehicle-treated HCR had higher NETO in skeletal muscle, BAT, and MWAT, consistent with previous baseline findings for skeletal muscle and BAT[13].

Intra-VMH MTII elevated expression of mRNA of mediators of energy expenditure

Levels of mRNA expression of potential molecular mediators of energy balance are shown in Table 2 and Figure 3. Compared to vehicle-treated HCR, gastrocnemius muscle of intra-VMH MTII-treated HCR had significantly higher mRNA expression of UCP2, UCP3, PGC-1α, PPARα, PPARδ, PPARγ, SERCA1, SERCA2, and β_2 AR, and a significant decrease in Kir6.2 (Figure 4A). Gastrocnemius showed a significantly higher expression of UCP2, UCP3, PPARα, PPARγ, and SERCA2 in MTII-treated LCR than vehicle-treated LCR. In quadriceps, MTII- and vehicle-microinjected HCR differed in mRNA expression (MTII>vehicle, within HCR) of UCP2, UCP3, PPARα, PPARδ, SERCA1, and SERCA2 (Figure 4B). MTII-treated LCR quadriceps showed significantly higher mRNA expression of UCP2 and UCP3 (Figure 4B) compared to vehicle-treated LCR quadriceps.

Compared to vehicle-treated rats, HCR but not LCR with intra-VMH MTII microinjections had significantly elevated mRNA expression of UCP1, PGC-1α, PPARδ, PPARγ, and PPARα in BAT (Table 2). Compared to vehicle, intra-VMH MTII also induced a significant increase in mRNA expression of PPARγ, PPARα, and PPARδ in WAT of intra-VMH MTII treated HCR where LCR showed MTII-induced increase in mRNA expression of PPARα and PPARδ in WAT. In liver, intra-VMH MTII-treated HCR showed significantly higher mRNA expression of UCP2, PPARα, PPARδ, PPARγ, and PGC-1α compared to vehicle-treated HCR. In LCR liver, MTII- and vehicle-treated rats significantly differed in mRNA expression of PPARα, PPARδ, PPARγ, and PGC-1α.

As shown in Table 3 and Figure S3, protein expression of mediators of EE did not consistently change in accordance with mRNA expression. In quadriceps, MTII-treated HCR only showed trends in pAMPK, pACC, PPARγ, and SERCA1. No significant differences or trends were found in protein expression with intra-VMH MTII in LCR. In gastrocnemius, intra-VMH MTII-microinjected HCR showed significantly higher expression of PGC-1α, pAMPK, and pACC compared to vehicle-treated HCR, with trends in other mediators; no significant differences were found in LCR (Figure S3).

As shown in Table 3 and Figure S3, in BAT of HCR, MTII-treated rats showed significantly higher UCP1, PGC-1α, pAMPK, and pACC. No significant differences were observed with MTII in LCR. No significant differences were observed with MTII in WAT except in pAMPK in MTII-treated HCR compared to vehicle-treated HCR. In liver, MTII-microinjected HCR showed significantly more pACC and pAMPK; no significant differences were observed in LCR.

DISCUSSION

Phenotypic leanness associated with high intrinsic aerobic capacity in rats is coupled with elevated total EE, and the predominant source of this is activity-related EE stemming from high daily physical activity along with low economy of activity in these rats[12,13]. This low muscle work efficiency suggests wasting of calories to a greater extent in HCR than LCR, potentially modulated by enhanced sympathetic drive and altered expression of molecular mediators of energy conservation and expenditure observed in HCR[13]. These phenotypic differences were similar to those seen in response to intra-VMH melanocortin receptor

activation[14], suggesting an elevated response of the melanocortinergic VMH-SNS-muscle axis in the lean HCR. Here, we identified a phenotype-linked increase in EE, physical activity, activity-associated EE, and VO_2 after site-specific activation of central melanocortin receptors. Many of these energetic changes were amplified in lean HCR compared to obesity-prone LCR; for example, VMH melanocortin receptor activation had a greater impact on EE and VO_2 in HCR (Figure 1), even taking into account differences in body weight and composition. The melanocortin receptor stimulation of EE during low- and moderate-intensity physical activity implicates mechanistic changes impacting muscle work efficiency, particularly in the lean HCR. This stems in part from enhanced central activation of SNS outflow to muscle. Elevated functioning of this brain-SNS-muscle axis in the high-capacity phenotype may be an important factor promoting aerobic capacity and potentially leanness.

Some thermogenic changes accompanied the MTII-induced increase in EE. BAT thermogenesis showed a short-term increase in freely moving MTII-treated rats (Figure S1). MTII enhanced treadmill-walking gastrocnemius muscle temperature, but contrary to expectation, obesity-prone LCR showed a greater response in their muscle heat dissipation during activity, approaching the level of vehicle-treated HCR (Figure 2). Prior reports indicate that during activity, EE and muscle thermogenesis rise alongside each other, are similarly enhanced by central stimuli[14], and are suppressed in concert after weight loss[26]. Muscle thermogenesis plateaus at relatively low levels of exertion[13,14,26,27]. This implies that, mechanistically, heat dissipation does not fully correspond to calorie use in muscle, particularly at higher workloads. Given the high muscle activity thermogenesis seen in HCR[13], central MTII may enhance EE without being reflected in further incremental increases in muscle temperature (i.e., subject to a ceiling effect). Our data also suggest that melanocortin stimulation can be used to enhance or normalize activity thermogenesis even in the obesity prone.

Activity thermogenesis and skeletal muscle metabolism are important in maintaining leanness[28], and this may be driven in part through central modulation. Evidence implicates a pathway through which the VMH and central melanocortin system integrate central and peripheral metabolic cues to meet muscle energy and glucose needs[15,16,29] though modulation of the SNS[16,30]. Here, we found that activation of VMH melanocortin receptors increased sympathetic outflow to peripheral metabolic systems in both HCR and LCR (Figure 3; Table 1). Moreover, in some muscle subgroups, NETO was significantly more enhanced by MTII in HCR compared to obesity-prone LCR. Differences in central autonomic regulation could therefore contribute to the overall higher SNS drive seen in the lean HCR[13]. The exception was the heart, where the MTII-induced increase in sympathetic outflow was higher in the LCR, and LCR showed higher NETO both with and without central melanocortin receptor stimulation (Figure 3). This corresponds with evidence that HCR are protected against hypertension[6] and with the role of melanocortin peptides and receptors in sympathetically driven hypertension and against the hypertensive effects of MTII[21,31,32]. The enhanced responsiveness of SNS outflow to muscle in HCR supports the idea that the amplified metabolic response to central melanocortins in HCR are due in part to higher SNS stimulation of muscle. This, along with muscle response to SNS signaling[33],

may underlie the phenotypic differences in fuel economy and the associated changes in cellular energy mediators in the periphery.

Overall, these findings affirmed our previous identification of phenotype-dependent differences in HCR and LCR[13] as well as muscle response to central melanocortin receptor activation[14]. Central melanocortin activation was effective in modulating mRNA expression in BAT and liver in both HCR and LCR (Figure 4, Table 2); here, we focus primarily on muscle, specifically on mediators of thermogenesis, fatty acid metabolism, and energy conservation. Potential thermogenic mediators SERCA1 & 2 and UCP2 & 3 showed induced mRNA expression in quadriceps and oxidative gastrocnemius muscle with central melanocortin stimulation, with some elevation seen in HCR and not LCR (gastrocnemius SERCA1, quadriceps SERCA 1 & 2; Table 3). Conversely, mRNA expression of MED1 and components of ATP-gated K^+ channels were higher in LCR muscle, potentially contributing to their overall lower muscle temperatures[35] and their energy conservation. Similar to previous reports[13,34], central melanocortin stimulation induced mRNA expression of PGC-1α, PPARα, PPARγ, and PPARδ in oxidative gastrocnemius muscle, and PPARα, PPARδ in quadriceps, with many of these significant in HCR but not LCR (Figure 4). These changes may be responsible for the central melanocortin receptor-induced increase in EE and decrease in RER. While the 4-hr time course of the study was optimal to detect increases in mRNA expression, it likely obscured detection of suppressive effects of central MTII beyond one instance (Kir6.2 in HCR gastrocnemius; Figure 4) and some statistical trends (PPARα, pAMPK, PPARγ and pACC; Table 3). Also, the time course did not allow for adequate time for detection of altered protein expression. Most of the changes identified were phosphorylation related and did not require translation. The expression of the activated form of AMPK (pAMPK) may underlie the ability of central MTII to upregulate fatty acid oxidation and reduce RER through its regulation of ACC and CPT1[36]. Lastly, both mRNA and protein expression reinforced our previous findings[13] showing baseline differences between HCR and LCR reflecting the observed phenotype-dependent differences in activity-related EE, RER, and muscle energy use. Taken together with the MTII-induced changes demonstrated here and the proposed melanocortin-activated VMH-SNS-muscle pathway, this suggests phenotypic differences in myocyte responsiveness to adrenergic stimuli, consistent with the findings of Lessard et al., 2009[33].

Altogether, our data demonstrate that melanocortin receptors in the VMH activate SNS outflow, increasing sympathetic drive to skeletal muscle, modulate fuel allocation and use through differential activation of molecular mediators of energy homeostasis, and increase EE while lowering fuel economy of activity. We have also demonstrated that functioning of this axis is heightened at every level in HCR compared to LCR—activation of melanocortin receptors in the VMH increases energy use in peripheral tissues including muscle, with a stronger effect in the high-capacity phenotype[13,14]. It is likely that muscle fuel uptake and utilization is modulated through the SNS, affecting skeletal muscle or other metabolically active tissues. The central melanocortin system, differentially expressed in the lean HCR and obese LCR, is known to impact muscle lipid mobilization and glucose uptake in the periphery via the SNS[15,17,19,20,37,38]. These findings support the importance of central modulation of SNS outflow to muscle in modulating activity EE, and suggest that differences in this pathway are linked to a high-aerobic capacity phenotype that shows

obesity resistance. We speculate that running capacity, leanness, and skeletal muscle energy use and thermogenesis are coupled mechanistically. These results implicate this pathway as a potential mechanism underlying high-endurance-associated low economy of activity and leanness, and may help identify potential mediators that can be targeted to alter energy balance equation towards negative energy balance.

Supplementary Material

Refer to Web version on PubMed Central for supplementary material.

Acknowledgments

We acknowledge the expert care of the rat colony provided by Lori Heckenkamp and Shelby Raupp. Contact LGK Lauren.Koch2@Utoledo.edu or SLB brittons@umich.edu for information on the LCR and HCR rats. We would like to thank Lydia Heemstra for organizing personnel, Amber Titus for a critical reading of the manuscript, and the staff of the animal care and housing at Kent State University for their support in taking care of the animals.

Funding: This work was funded by National Institutes of Health (NIH) grants NIH R01NS055859 and NIH R15DK097644, as well as American Heart Association grant 12GRNT12050566 to CMN. The LCR-HCR rat model system was funded by the Office of Research Infrastructure Programs grant P40OD021331 (to LGK and SLB) from the National Institutes of Health.

References

1. Joosen AM, Gielen M, Vlietinck R, Westerterp KR. Genetic analysis of physical activity in twins. Am J Clin Nutr. 2005; 82(6):1253–1259. [PubMed: 16332658]
2. Levine JA, Kotz CM. NEAT–non-exercise activity thermogenesis–egocentric & geocentric environmental factors vs. biological regulation Acta Physiol Scand. 2005; 184(4):309–318. [PubMed: 16026422]
3. Levine JA, Lanningham-Foster LM, McCrady SK, et al. Interindividual variation in posture allocation: possible role in human obesity. Science. 2005; 307(5709):584–586. [PubMed: 15681386]
4. Aspenes ST, Nilsen TI, Skaug EA, Bertheussen GF, Ellingsen O, Vatten L, Wisloff U. Peak oxygen uptake and cardiovascular risk factors in 4631 healthy women and men. Med Sci Sports Exerc. 2011; 43(8):1465–1473. [PubMed: 21228724]
5. Bray MS. Genomics, genes, and environmental interaction: the role of exercise. J Appl Physiol. 2000; 88(2):788–792. [PubMed: 10658051]
6. Koch LG, Britton SL, Wisloff U. A rat model system to study complex disease risks, fitness, aging, and longevity. Trends Cardiovasc Med. 2012; 22(2):29–34. [PubMed: 22867966]
7. Kodama S, Saito K, Tanaka S, Maki M, et al. Cardiorespiratory fitness as a quantitative predictor of all-cause mortality and cardiovascular events in healthy men and women: a meta-analysis. JAMA. 2009; 301(19):2024–2035. [PubMed: 19454641]
8. Novak CM, Escande C, Gerber SM, et al. Endurance capacity, not body size, determines physical activity levels: role of skeletal muscle PEPCK. PLoSONE. 2009; 4:e5869.
9. Zhan WZ, Swallow JG, Garland T Jr, Proctor DN, Carter PA, Sieck GC. Effects of genetic selection and voluntary activity on the medial gastrocnemius muscle in house mice. J Appl Physiol. 1999; 87(6):2326–2333. [PubMed: 10601185]
10. Kokkinos P, Myers J, Kokkinos JP, et al. Exercise capacity and mortality in black and white men. Circulation. 2008; 117:614–622. [PubMed: 18212278]
11. Myers J, Prakash M, Froelicher V, Do D, Partington S, Atwood JE. Exercise capacity and mortality among men referred for exercise testing. N Engl J Med. 2002; 346:793–801. [PubMed: 11893790]
12. Novak CM, Escande C, Burghardt PR, et al. Spontaneous activity, economy of activity, and resistance to diet-induced obesity in rats bred for high intrinsic aerobic capacity. Horm Behav. 2010; 58(3):355–367. [PubMed: 20350549]

13. Gavini CK, Mukherjee S, Shukla C, Britton SL, Koch LG, Shi H, Novak CM. Leanness and Heightened Non-Resting Energy Expenditure: Role of Skeletal Muscle Activity Thermogenesis. Am J Physiol Endocrinol Metab. 2014; 306(6):E635–47. [PubMed: 24398400]
14. Gavini CK, Jones WC II, Novak CM. Ventromedial hypothalamic melanocortin receptor activation: regulation of activity energy expenditure and skeletal muscle thermogenesis. J Physiol. 2016; 594:5285–5301. [PubMed: 27126579]
15. Toda C, Shiuchi T, Lee S, et al. Distinct effects of leptin and a melanocortin receptor agonist injected into medial hypothalamic nuclei on glucose uptake in peripheral tissues. Diabetes. 2009; 58:2757–65. [PubMed: 19752162]
16. Shiuchi T, Haque MS, Okamoto S, et al. Hypothalamic orexin stimulates feeding-associated glucose utilization in skeletal muscle via sympathetic nervous system. Cell Metab. 2009; 10:466–480. [PubMed: 19945404]
17. Tanaka T, Masuzaki H, Yasue S, et al. Central melanocortin signaling restores skeletal muscle AMP-activated protein kinase phosphorylation in mice fed a high-fat diet. Cell Metab. 2007; 5:395–402. [PubMed: 17488641]
18. Miyaki T, Fujikawa T, Kitaoka R, Hirano N, Matsumura S, Fushiki T, Inoue K. Noradrenergic projections to the ventromedial hypothalamus regulate fat metabolism during endurance exercise. Neuroscience. 2011; 190:239–50. [PubMed: 21640797]
19. Shukla C, Britton SL, Koch LG, Novak CM. Region-specific differences in brain melanocortin receptors in rats of the lean phenotype. Neuroreport. 2012; 23:596–600. [PubMed: 22643233]
20. Shukla C, Koch LG, Britton SL, Cai M, Hruby VJ, Bednarek M, Novak CM. Contribution of regional brain melanocortin receptor subtypes to elevated activity energy expenditure in lean, active rats. Neuroscience. 2015; 310:252–67. [PubMed: 26404873]
21. Rahmouni K, Haynes WG, Morgan DA, Mark AL. Role of melanocortin-4 receptors in mediating renal sympathoactivation to leptin and insulin. J Neurosci. 2003; 23:5998–6004. [PubMed: 12853417]
22. Schoeller DA, Jefford G. Determinants of the energy costs of light activities: inferences for interpreting doubly labeled water data. Int J Obes Relat Metab Disord. 2002; 26(1):97–101. [PubMed: 11791153]
23. Tschöp MH, Speakman JR, Arch JR, et al. A guide to analysis of mouse energy metabolism. Nat Methods. 2012; 9:57–63.
24. Shi H, Bowers RR, Bartness TJ. Norepinephrine turnover in brown and white adipose tissue after partial lipectomy. Physiol Behav. 2004; 81:535–42. [PubMed: 15135027]
25. Vaughan CH, Shrestha YB, Bartness TJ. Characterization of a novel melanocortin receptor-containing node in the SNS outflow circuitry to brown adipose tissue involved in thermogenesis. Brain Res. 2011; 1411:17–27. [PubMed: 21802070]
26. Almundarij TI, Gavini CK, Novak CM. Suppressed sympathetic outflow to skeletal muscle, muscle thermogenesis, and activity energy expenditure with calorie restriction. Physiol Rep. 2017 Feb.5(4) pii:e13171.
27. Yoo Y, LaPradd M, Kline H, et al. Exercise activates compensatory thermoregulatory reaction in rats: a modeling study. J Appl Physiol. 2015; 119(12):1400–10. [PubMed: 26472864]
28. Jensen MD. Fatty acid oxidation in human skeletal muscle. J Clin Invest. 2002; 110:1607–1609. [PubMed: 12464664]
29. Braun TP, Marks DL. Hypothalamic regulation of muscle metabolism. Curr Opin Clin Nutr Metab Care. 2011; 14(3):237–242. [PubMed: 21502918]
30. Lindberg D, Chen P, Li C. Conditional viral tracing reveals that steroidogenic factor 1-positive neurons of the dorsomedial subdivision of the ventromedial hypothalamus project to autonomic centers of the hypothalamus and hindbrain. J Comp Neurol. 2013; 521(14):3167–3190. [PubMed: 23696474]
31. da Silva AA, do Carmo JM, Kanyicska B, Dubinion J, Brandon E, Hall JE. Endogenous melanocortin system activity contributes to the elevated arterial pressure in spontaneously hypertensive rats. Hypertension. 2008; 51(4):884–890. [PubMed: 18285617]

32. Haynes WG, Morgan DA, Djalali A, Sivitz WI, Mark AL. Interactions between the melanocortin system and leptin in control of sympathetic nerve traffic. Hypertension. 1999; 33(1 Pt 2):542–547. [PubMed: 9931162]

33. Lessard SJ, Rivas DA, Chen ZP, et al. Impaired skeletal muscle beta-adrenergic activation and lipolysis are associated with whole-body insulin resistance in rats bred for low intrinsic exercise capacity. Endocrinology. 2009; 150(11):4883–4891. [PubMed: 19819977]

34. Overmyer KA, Evans CR, Qi NR, et al. Maximal oxidative capacity during exercise is associated with skeletal muscle fuel selection and dynamic changes in mitochondrial protein acetylation. Cell metab. 2015; 21:468–478. [PubMed: 25738461]

35. Alekseev AE, Reyes S, Yamada S, et al. Sarcolemmal ATP-sensitive K(+) channels control energy expenditure determining body weight. Cell Metab. 2010; 11(1):58–69. [PubMed: 20074528]

36. Minokoshi Y, Kim YB, Peroni OD, Fryer LG, Muller C, Carling D, Kahn BB. Leptin stimulates fatty-acid oxidation by activating AMP-activated protein kinase. Nature. 2002; 415(6869):339–343. [PubMed: 11797013]

37. Nogueiras R, Wiedmer P, Perez-Tilve D, et al. The central melanocortin system directly controls peripheral lipid metabolism. J Clin Invest. 2007; 117(11):3475–3488. [PubMed: 17885689]

38. Sohn JW, Harris LE, Berglund ED, et al. Melanocortin 4 receptors reciprocally regulate sympathetic and parasympathetic preganglionic neurons. Cell. 2013; 152(3):612–619. [PubMed: 23374353]

STUDY IMPORTANCE

- Intra-ventromedial hypothalamic melanocortin receptor activation increases physical activity and energy expenditure
- Here, we demonstrate that this response is enhanced in inherently lean rats
- Intrinsic differences in brain melanocortins and sympathetic outflow to muscle may underlie the elevated activity energy expenditure seen in leanness

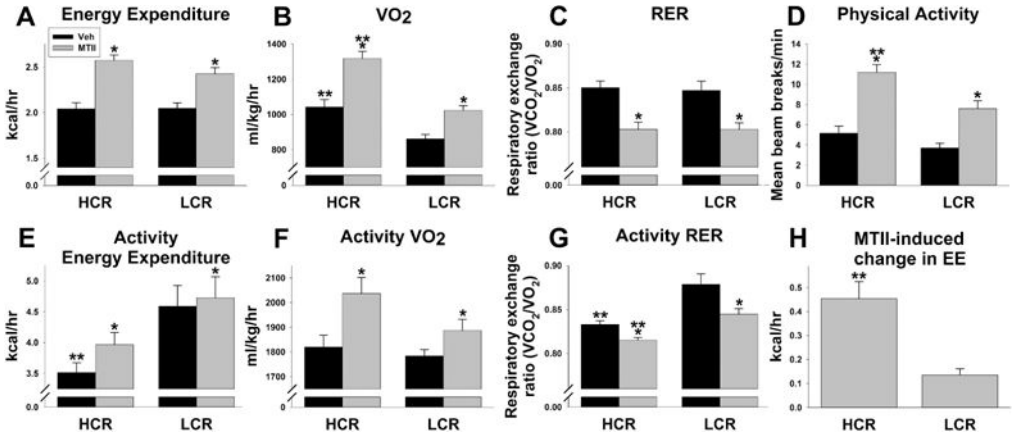

Figure 1.

High-capacity runners (HCR) were more responsive to the ability of intra-ventromedial hypothalamic (VMH) melanocortin receptor activation to enhance activity-related energy expenditure (EE). Low-capacity runners (LCR) and HCR were given intra-VMH microinjections of the mixed melanocortin receptor agonist Melanotan II (MTII; gray bars) or vehicle (Veh; black bars). Over 4 hours, with a significant interaction where HCR responded more than LCR, intra-VMH MTII significantly increased free-moving EE (A), VO_2 (B), and physical activity (D), while decreasing respiratory exchange ratio (RER) similarly in HCR and LCR (C). (E–H) Intra-VMH MTII also induced changes in EE and RER in rats walking on a treadmill at 7 meters/min for 30 min. MTII increased activity-associated EE (E) and VO_2 (F), and decreased RER (G) in HCR and LCR. HCR showed lower overall walking-induced RER, while intra-VMH MTII produced a larger RER decrease in LCR than HCR (G), whereas HCR were more responsive to MTII-induced enhancement of activity EE (H). *within group, MTII treatment significantly different from veh; **HCR significantly different from LCR within treatment; $p<0.05$. (N=10)

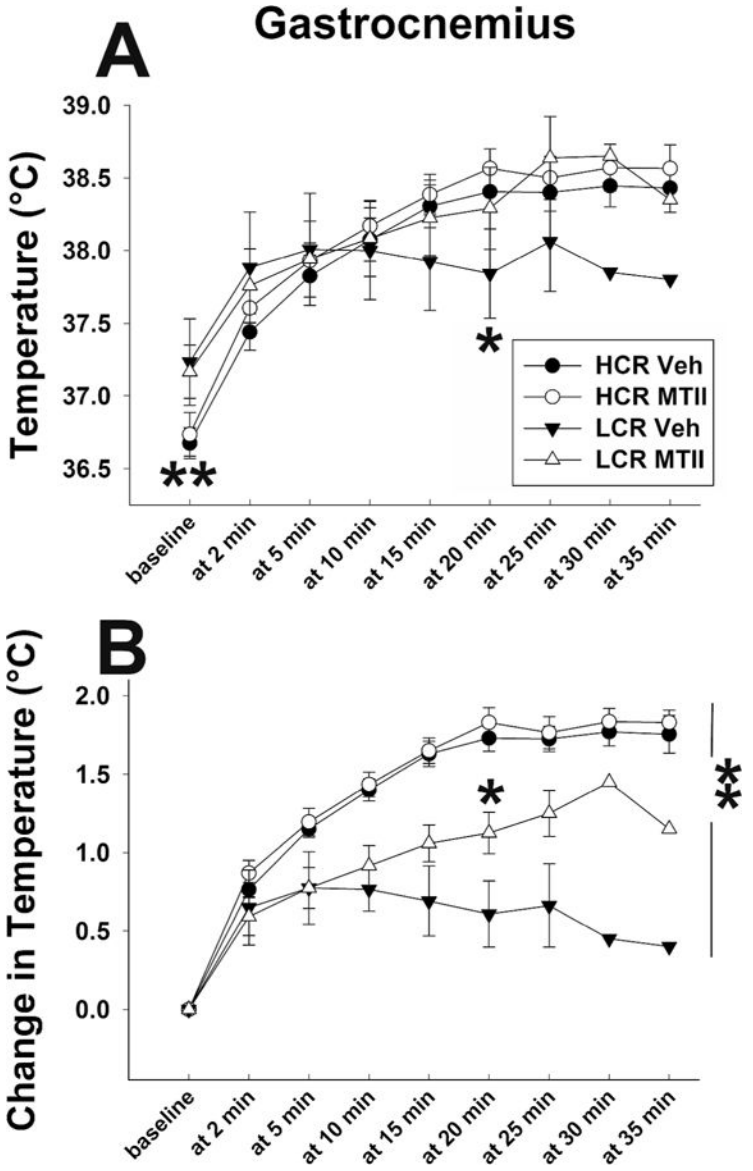

Figure 2.

(A) Low and moderate intensity treadmill activity increased skeletal muscle (gastrocnemius) temperature in high-capacity runners (HCR; circles) and low-capacity runners (LCR; triangles) after intra-ventromedial hypothalamic (VMH) microinjections of the mixed melanocortin receptor agonist Melanotan II (MTII; open symbols) or vehicle (Veh; filled symbols). (B) Walking-induced increases in muscle temperature from baseline were significantly higher in HCR, whereas intra-VMH MTII significantly increased activity-associated muscle heat dissipation in LCR but not HCR. *LCR, MTII treatment significantly different from Veh; ** HCR > LCR, main effect (A) and difference at baseline (B); $p<0.05$. (N=10/HCR, 6/LCR)

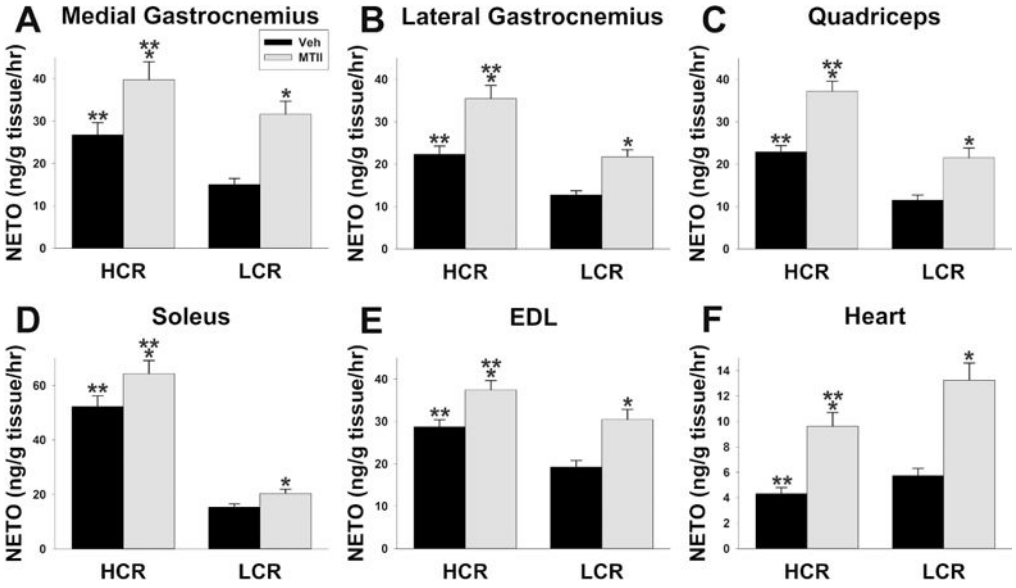

Figure 3.

Norepinephrine turnover (NETO) showed differences in sympathetic drive in high- and low-capacity runners (HCR. LCR) after intra-ventromedial hypothalamic (VMH) microinjections of the mixed melanocortin receptor agonist Melanotan II (MTII; gray bars) or vehicle (Veh; black bars). Intra-VMH MTII significantly increased NETO in skeletal muscle including (A) medial gastrocnemius, (B) lateral gastrocnemius, (C) quadriceps, (D) soleus, and (E) extensor digitorum longus (EDL); HCR showed significantly higher NETO in each of these muscle groups, and also had significantly greater MTII-induced NETO in lateral gastrocnemius, quadriceps, and soleus (line × treatment interaction). (F) Intra-VMH MTII also increased NETO in heart, but here the MTII-induced increase was greater in LCR than HCR. *within group, MTII treatment significantly different from veh; **HCR significantly different from LCR within treatment; $p<0.05$. (N=7-HCR, 8-LCR)

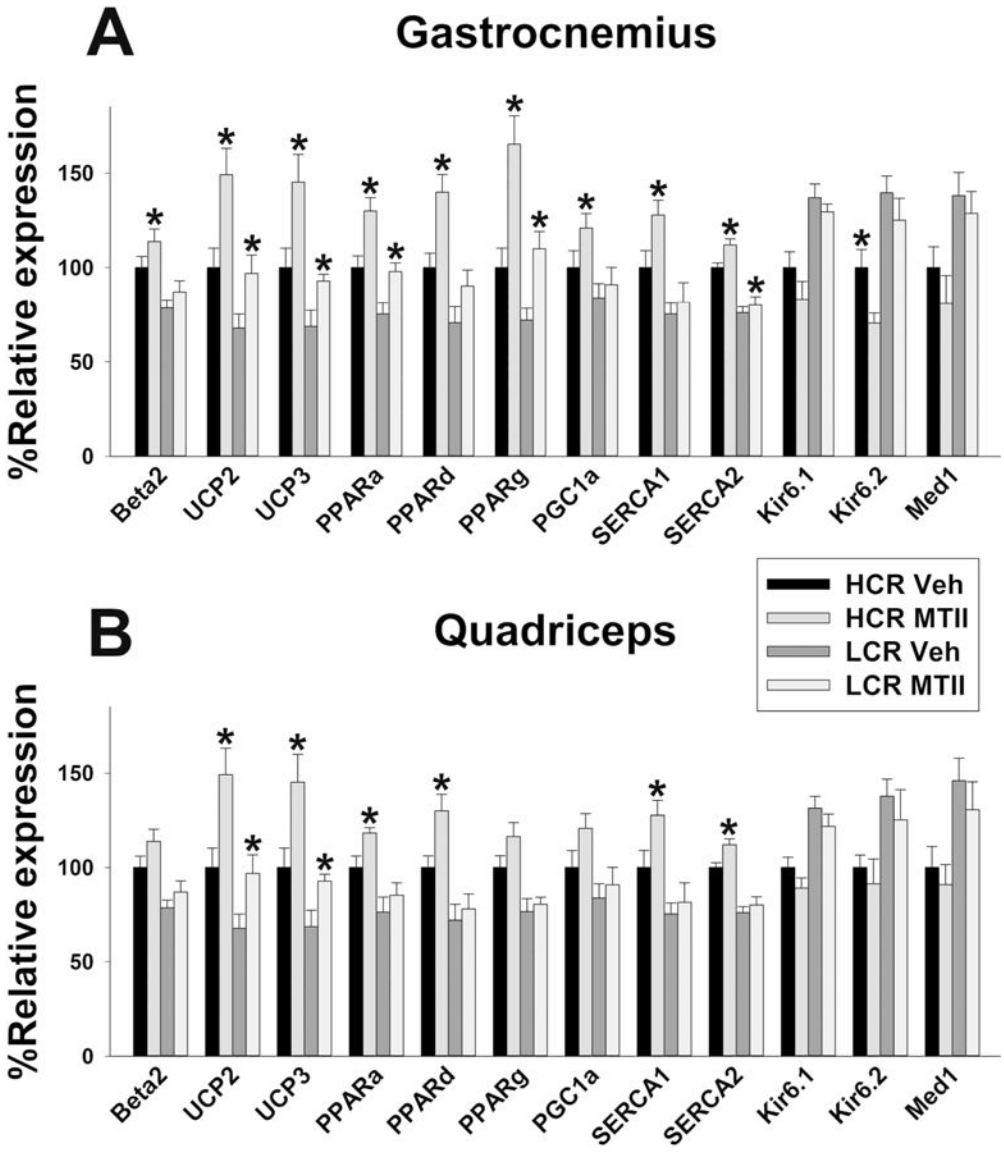

Figure 4.

Intra-ventromedial hypothalamic (VMH) microinjections of the Melanotan II (MTII) altered mRNA expression of energetic mediators in skeletal muscle (A: medial gastrocnemius; B: quadriceps) in high-and low-capacity runners (HCR, LCR). Beta2: β2 adrenergic receptor; UCP2 and 3: uncoupling protein 2 and 3; PPARa, d, and g: peroxisome proliferator-activated receptor α, δ, and γ; SERCA 1 and 2: sarco/endoplasmic reticulum ATPase 1 and 2; Kir6.1 and 6.2 subunits of the ATP-gated K^+ channel, Med1: mediator of RNA polymerase II transcription subunit 1. HCR MTII ≠ LCR MTII in all cases. *within group, MTII treatment significantly different from veh; $p<0.05$. (N=8-group)

Table 1

Norepinephrine turnover (ng NE/g tissue/hr) in high-capacity runners (HCR) and low-capacity runners (LCR) 4 hrs after intra-ventromedial hypothalamic microinjection of either the mixed melanocortin receptor agonist MTII or vehicle. Mean±SEM

Tissue		HCR		LCR	
		vehicle	MTII*	vehicle	MTII*
White adipose tissue	Mesenteric†**	18.88 ** ± 2.30	38.73 ** ± 4.72	8.39 ± 0.71	15.24 ± 1.30
	Retroperitoneal	8.04 ± 0.70	13.99 ± 1.23	6.32 ± 0.87	11.34 ± 1.56
	Epididymal†**	5.22 ** ± 0.60	7.58 ** ± 0.87	2.05 ± 0.11	5.56 ± 0.31
	Gluteal†**	4.92 ± 0.30	7.95 ** ± 0.49	4.19 ± 0.37	4.52 ± 0.40
	Inguinal†**	2.29 ± 0.19	3.88 ** ± 0.32	1.90 ± 0.17	2.43 ± 0.22
Brown adipose tissue†**		27.45 ** ± 1.54	62.50 ** ± 3.51	18.36 ± 1.06	30.91 ± 1.78
Liver†		0.85 ± 0.10	2.11 ** ± 0.26	0.66 ± 0.06	1.17 ± 0.10

HCR, high-capacity runners; LCR, low-capacity runners (N=7/HCR, 8/LCR)

*MTII>vehicle, within line (HCR/LCR) when interaction was significant; all tissues showed main effect of MTII; $p<0.05$

**HCR≠LCR within treatment indicated; main effect of line (HCR/LCR) indicated on tissue; $p<0.05$

†Significant interaction between treatment (vehicle/MTII) and line (HCR/LCR); $p<0.05$

Table 2

Changes in relative mRNA expression after intra-ventromedial hypothalamic treatment with the melanocortin receptor agonist MTII. In percent of vehicle-treated HCR, mean±SEM

Tissue		HCR		LCR	
		vehicle	MTII	vehicle	MTII
Brown Adipose Tissue	B3-AR	100.0±7.6	101±12.8	80.3±5.2	89.6±10.7
	UCP1 *,**	100.0±5.1	129±5.1	65.9±7.9	82.6±5.4
	PPARα *,**	100.0±7.1	132±5.8	73.8±6.5	90.7±7.9
	PPARδ **	100.0±8.0	133±5.5	71.8±6.1	87.7±5.8
	PPARγ *,**	100.0±2.0	123±4.7	79.6±4.3	92.7±5.9
	PGC-1α *,**	100.0±9.6	144±10.5	68.3±9.4	89.2±7.9
White Adipose Tissue	B3-AR *,**	100.0±6.3	116.0±10.5	76.9±7.4	85.9±5.5
	UCP2 **	100.0±8.9	110.6±8.3	67.9±7.5	73.9±8.7
	PPARα *,**	100.0±5.5	132.4±7.3	67.9±7.9	91.6±4.1
	PPARδ *,**	100.0±9.7	136.5±5.7	65.0±10.1	97.3±7.5
	PPARγ *,**	100.0±8.1	129.7±8.5	72.5±6.9	89.1±8.4
	PGC-1α **	100.0±5.2	112.9±7.6	70.9±9.6	75.6±8.8
Liver	B2-AR *,**	100.0±7.8	117.6±6.9	75.5±5.7	95.4±9.9
	UCP2 *,**	100.0±5.3	129.9±8.4	79.5±6.4	95.9±9.8
	PPARα *,**	100.0±8.2	149.7±10.8	78.3±7.0	109.6±6.8
	PPARδ *,**†	100.0±6.2	172.2±7.2	72.4±7.0	111.0±9.6
	PPARγ *,**	100.0±9.5	164.5±15.4	76.2±5.9	115.0±3.5
	PGC-1α *,**	100.0±4.7	159.8±9.8	72.0±6.0	113.0±8.9

HCR, high-capacity runners; LCR, low-capacity runners; B2-AR, beta-2 adrenergic receptor; B3-AR, beta-3 adrenergic receptor; PPAR, peroxisome proliferator activated protein; PGC-1α, PPARγ coactivator-1α; UCP, uncoupling protein.

*MTII>vehicle;

**HCR≠LCR

† Significant interaction between treatment (vehicle/MTII) and line (HCR/LCR); $p<0.05$. (N=8/group)

Table 3

Changes in relative protein level after intra-ventromedial hypothalamic treatment with the melanocortin receptor agonist MTII. In percent of vehicle-treated HCR, or as a ratio to unphosphorylated protein, mean±SEM.

Tissue		HCR		LCR	
		vehicle	MTII	vehicle	MTII
Gastrocnemius	B2-AR**	100.0±5.7	111.6±5.9	80.0±5.2	85.7±5.2
	UCP2*,**	100.0±6.3	108.0±6.4	75.4±6.1	78.6±5.5
	UCP3*,**	100.0±5.6	111.4±5.8	74.0±6.2	77.0±5.4
	PPARα**	100.0±5.2	110.0±6.1	79.7±5.2	85.3±5.4
	PPARδ**	100.0±5.9	113.0±6.4	76.5±5.6	86.0±6.8
	PPARγ**	100.0±5.4	116.7±6.4	77.4±5.5	85.3±5.3
	PGC-1α*,**	100.0±5.6	121.6±4.8	71.7±5.4	79.3±5.2
	CPT1	100.0±6.5	111.7±6.0	89.6±6.0	96.9±5.4
	SERCA1*,**	100.0±4.9	116.5±5.8	74.9±5.2	84.0±6.7
	SERCA2**	100.0±6.0	115.9±5.2	69.5±5.2	74.4±5.6
	Kir6.1**	100.0±4.7	97.7±5.6	119.7±4.3	118.0±7.9
	Kir6.2**	100.0±5.9	97.3±4.8	129.7±5.4	129.5±5.7
	MED1**	100.0±5.0	99.9±5.4	131.7±5.6	128.9±5.9
	FAS	100.0±5.7	97.9±5.4	92.6±5.9	92.4±6.0
	CD36 (FAT)**	100.0±6.2	111.0±5.8	82.0±5.4	87.9±6.6
	ACC	100.0±5.4	99.8±5.5	107.9±5.7	104.4±5.5
	pACC*,**	100.0±5.2	121.4±4.9	78.2±5.4	89.5±5.8
	pACC/ACC*,**	100.2±4.5	122.3±5.5	73.0±7.6	87.3±9.8
	AMPK	100.0±5.4	100.5±5.0	99.9±5.7	99.4±5.5
	pAMPK*,**	100.0±5.2	122.0±4.5	97.2±5.5	91.6±5.4
	pAMPK/AMPK*,**	100.4±6.3	123.0±10.6	79.6±6.1	92.2±3.4
Quadriceps	B2-AR**	100.0±6.7	105.9±6.9	83.7±5.2	87.5±6.7

Tissue		HCR		LCR	
		vehicle	MTII	vehicle	MTII
Brown Adipose Tissue	UCP2**	100.0±6.1	106.6±7.0	74.4±6.4	76.6±5.4
	UCP3**	100.0±5.7	108.4±5.9	73.0±6.8	75.5±5.8
	PPARα**	100.0±	108.0±8.2	85.0±7.4	89.0±5.9
	PPARδ**	100.0±	102.5±6.9	85.5±5.4	84.7±7.8
	PPARγ**	100.0±	112.5±6.5	83.7±5.4	89.1±5.8
	PGC-1α**	100.0±5.3	111.9±5.2	70.2±5.8	76.3±5.9
	CPT1	100.0±6.5	109.9±6.0	92.6±5.7	102.9±5.4
	SERCA1**	100.0±4.9	114.8±5.8	78.5±5.2	87.0±6.7
	SERCA2**	100.0±5.0	110.9±5.2	76.5±5.7	83.7±6.6
	Kir6.1	100.0±5.7	98.3±5.8	112.9±4.2	109.5±6.9
	Kir6.2**	100.0±4.9	96.7±5.9	126.8±4.4	123.2±5.9
	MED1**	100.0±4.7	98.7±5.8	129.8±5.9	127.0±5.0
	FAS	100.0±6.0	98.7±6.4	98.4±5.6	99.4±6.6
	CD36 (FAT)**	100.0±7.2	103.0±6.1	95.8±6.1	86.4±7.6
	ACC	100.0±6.5	99.0±6.0	106.6±5.7	102.9±5.4
	pACC**	100.0±6.0	113.8±4.8	89.4±5.8	96.4±5.9
	pACC/ACC**	100.8±8.1	117.1±11.3	85.3±9.1	93.4±3.3
	AMPK	100.0±7.5	99.5±7.6	99.8±6.8	99.4±5.5
	pAMPK*,**	100.0±5.0	117.0±4.6	98.6±5.5	89.7±5.3
	pAMPK/AMPK**	100.6±7.3	118.2±7.7	79.3±6.7	90.6±5.9
	B3-AR**	100.0±6.3	107.4±8.0	76.3±5.5	88.9±7.8
	UCP1*,**	100.0±3.9	119.4±4.0	65.8±4.9	76.2±3.5
	PPARα	100.0±7.4	115.0±9.8	88.2±8.7	95.7±5.6
	PPARδ	100.0±5.9	107.9±6.7	93.8±4.3	98.8±7.5
	PPARγ**	100.0±4.6	106.5±6.8	78.2±6.3	87.9±7.7

Tissue		HCR		LCR	
		vehicle	MTII	vehicle	MTII
White Adipose Tissue	PGC-1α[*,**]	100.0±5.4	123.2±6.0	78.0±4.3	85.1±7.2
	CPT1	100.0±6.5	112.8±5.3	78.6±5.4	90.4±7.3
	FAS	100.0±6.3	98.9±5.0	100.9±4.8	99.8±5.8
	CD36 (FAT)[**]	100.0±9.1	102.6±7.3	90.5±6.5	95.4±6.2
	ACC	100.0±7.3	99.5±6.7	103.7±5.7	104.2±7.6
	pACC[*,**]	100.0±4.3	126.8±7.1	89.4±6.0	99.8±5.3
	pACC/ACC[*,**]	100.5±5.8	127.3±1.5	86.4±3.8	97.6±9.9
	AMPK	100.0±6.5	98.6±5.3	101.7±3.8	100.4±7.3
	pAMPK[*,**]	100.0±5.9	138.7±7.3	79.9±5.7	97.3±7.3
	pAMPK/AMPK[*,**]	100.8±8.4	141.8±11.2	76.9±3.9	97.5±4.0
	B3-AR[**]	100.0±5.5	109.0±6.0	80.6±4.6	86.0±6.6
	UCP2[**]	100.0±5.3	106.0±4.4	89.3±4.8	92.7±5.6
	PPARα	100.0±5.3	111.6±5.9	86.4±6.1	94.2±6.9
	PPARδ	100.0±3.5	106.6±4.2	92.8±4.9	99.5±3.7
	PPARγ	100.0±6.5	102.7±8.2	98.6±5.9	100.9±6.4
	PGC-1α[**]	100.0±5.9	111.4±6.5	91.8±4.4	99.3±7.2
	FAS	100.0±7.6	96.4±7.3	101.9±5.9	99.8±6.2
	CD36 (FAT)	100.0±5.8	99.6±6.5	104.3±6.8	104.1±5.3
	ACC	100.0±6.3	99.9±5.8	104.4±6.2	103.9±6.2
	pACC	100.0±5.8	112.0±4.4	93.8±5.7	105.4±5.7
	pACC/ACC	100.3±2.1	112.9±6.5	90.7±8.9	102.1±7.5
	AMPK	100.0±5.8	99.8±4.2	100.8±5.4	99.9±5.4
	pAMPK[*]	100.0±5.9	122.7±5.0	98.1±5.6	107.9±5.6
	pAMPK/AMPK	100.7±9.3	125.1±11.1	98.4±8.4	108.3±2.9
Liver	B2-AR[**]	100.0±5.0	105.8±6.9	80.4±5.4	89.5±5.5
	UCP2[**]	100.0±5.1	109.8±5.9	79.9±4.6	86.5±5.2

Tissue		HCR		LCR	
		vehicle	MTII	vehicle	MTII
	PPARα	100.0±6.9	113.6±5.7	89.3±5.4	99.1±4.9
	PPARδ**	100.0±6.3	117.6±6.4	83.7±5.2	91.7±5.6
	PPARγ**	100.0±5.4	115.4±5.9	76.8±5.7	85.2±6.3
	PGC-1α**	100.0±5.8	108.4±4.9	86.5±4.8	87.2±5.7
	CPT1	100.0±5.2	105.3±6.4	88.7±5.2	97.0±4.0
	FAS	100.0±5.5	98.5±6.1	100.8±5.2	101.7±5.8
	CD36 (FAT)**	100.0±4.0	95.7±5.4	111.5±4.9	109.8±4.8
	ACC	100.0±6.2	99.5±5.3	104.8±5.2	105.7±6.7
	pACC	100.0±5.4	125.4±6.8	89.3±5.5	94.2±6.7
	pACC/ACC**	101.2±10.5	126.7±2.1	86.6±9.1	90.0±7.5
	AMPK	100.0±5.9	100.0±6.0	100.3±6.1	100.5±5.4
	pAMPK*,**	100.0±5.2	122.7±5.4	89.7±5.2	95.8±5.0
	pAMPK/AMPK**	100.2±4.9	123.1±4.4	90.0±8.4	96.7±10.4

HCR, high-capacity runners; LCR, low-capacity runners; B2-AR, beta-2 adrenergic receptor; B3-AR, beta-3 adrenergic receptor; PPAR, peroxisome proliferator activated protein; PGC-1α, PPARγ coactivator-1α; UCP, uncoupling protein; CPT1, carnitine-palmitoyl transferase 1; SERCA, sarcoplasmic-endoplasmic reticulum calcium ATPase; Kir, inwardly-rectifying potassium channel; MED1, Mediator of RNA polymerase II transcription subunit 1; FAS, fatty acid synthase; CD36/FAT, cluster of differentiation 36/fatty acid translocase; ACC, acetyl-CoA carboxylase; AMPK, AMP-activated protein kinase.

*MTII>vehicle;

**HCR≠LCR; p<0.05